Physics – Uspekhi **53** (7) 677 – 689 (2010)

REVIEWS OF TOPICAL PROBLEMS PACS numbers: 75.30.Kz, **75.40. – s**, 75.50.Ee, 75.60.Ch, **75.70. – i**

Surface spin-flop transition in an antiferromagnet

A I Morosov, A S Sigov

DOI: 10.3367/UFNe.0180.201007b.0709

Contents

Abstract. Surface spin-flop transition is investigated for smooth and rough uncompensated surfaces of a semi-infinite, two-sublattice, collinear antiferromagnet. The influence of size effects arising in the flat antiferromagnetic layer on the spin-flop and spin-flip transitions is considered for smooth and rough surfaces. A principal difference is demonstrated between how the spin-flop transition proceeds in the layer areas with an odd and even number of atomic planes.

1. Introduction

The physical properties of a crystal near the surface are known to differ from those in the bulk. This difference makes possible phase transitions near the surface at the temperature, external field strength or a value of other governing parameter, the values of which do not correspond to the phase transition point in an infinite crystal.

An example of such a difference is the spin-flop transition in a two-sublattice uniaxial collinear antiferromagnet in a magnetic field applied along the easy axis. It should be noted that theoretical models of surface transitions described in the literature as a rule consider flat smooth crystal surfaces. The real surface of a crystal always contains atomic steps that change the coordinate corresponding to the flat surface by the height of a single atomic layer. Atomic steps present on an uncompensated antiferromagnetic surface break it down into regions of two types, in which the magnetization vector of the upper atomic layer is parallel and antiparallel to the external magnetic field, respectively. Scenarios of spin-flop transition in regions of different types also depend on the relationship between the correlation radius of the antiferromagnetic order parameter and the region size. Investigation into these scenarios are the primary objective of this review.

Its secondary objective is to consider spin-flop and spin-flip transitions in plane-parallel antiferromagnetic layers a nanometer thick under conditions in which the correlation radius of the order parameter compares with the layer thickness and size effects become essential. The model of the plane-parallel antiferromagnetic layer fairly well describes antiferromagnetic atomic chains at the ferromagnet surface and multilayer magnetic structures with antiferromagnetic interaction between adjacent ferromagnetic layers. Such multilayer structures exhibiting giant magnetoresistance effect have proved to be of great interest for researchers and practising engineers which justifies the appearance of the present review.

L Néel was the first to predict spin-flop transition in the bulk of an infinite antiferromagnet [1]. Let us consider a system of quasiclassical localized spins for temperature $T \ll T_{\mathrm{N}}$ (where T_{N} is the Néel temperature), where localized spin moduli may be regarded as constant. The exchange interaction energy in the approximation of nearest neighbor interactions has the form

$$W_{\mathrm{ex}} = -\frac{1}{2}\,\tilde{z}JN\cos\psi\,, \tag{1}$$

where $\tilde{z}$ is the number of nearest neighbors, $J<0$ is the exchange integral, with spin values being included in the corresponding constants (in the present case, in J), N is the number of spins, and ψ is the angle between sublattice magnetizations.

The energy of single-ion anisotropy is given by

$$W_{\mathrm{an}} = -\frac{N}{2}\sum_{i=1}^{2} K\cos^2\varphi_i\,, \tag{2}$$

where $K>0$ is the anisotropy constant, φ_i is the angle between magnetization of the ith sublattice ($i=1,2$) and the easy x-axis (Fig. 1a), and $\psi=\varphi_1-\varphi_2$.

A I Morosov, A S Sigov Moscow State Institute of Radioengineering, Electronics and Automation (Technical University), prosp. Vernadskogo 78, 119454 Moscow, Russian Federation
Tel. (7-495) 433 03 11, (7-495) 433 00 44 . Fax (7-495) 434 86 65
E-mail: morosov@mirea.ru, rector@mirea.ru

Received 30 September 2009, revised 19 February 2010
Uspekhi Fizicheskikh Nauk **180** (7) 709 – 722 (2010)
DOI: 10.3367/UFNr.0180.201007b.0709
Translated by Yu V Morozov; edited by A Radzig

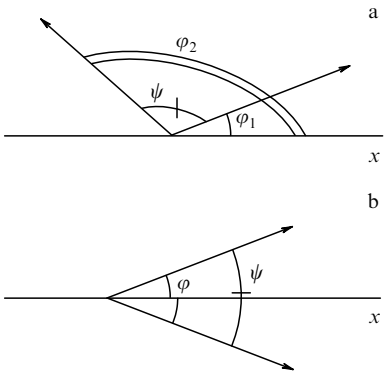

Figure 1. (a) Angles φ_1 and φ_2 characterizing directions of magnetization vectors of antiferromagnetic sublattices, $\psi = \varphi_1 - \varphi_2$. (b) Orientation of magnetization vectors in the spin-flop phase.

The energy of spins in the external magnetic field parallel to the easy axis is expressed as

$$W_B = -\mu B_0 \frac{N}{2} \sum_{i=1}^{2} \cos \varphi_i \,, \tag{3}$$

where μ is the atomic magnetic moment, and B_0 is the induction of the external magnetic field.

In the collinear phase, where $\varphi_1 = 0$, $\varphi_2 = \pi$, the total energy $W = W_{ex} + W_{an} + W_B$ equals [1]

$$W_1 = -\left(\frac{1}{2}\,\tilde{z}|J| + K\right)N. \tag{4}$$

In the spin-flop phase (Fig. 1b), $\varphi_1 = -\varphi_2 = \varphi$, and the total energy W takes the form

$$W_2 = -\left(\frac{1}{2}\,\tilde{z}J\cos 2\varphi + K\cos^2\varphi + \mu B_0 \cos\varphi\right)N. \tag{5}$$

Minimizing W_2 over φ and introducing notations

$$\alpha = \frac{K}{\tilde{z}|J|} \ll 1 \,, \tag{6}$$

$$\beta = \frac{\mu B_0}{\tilde{z}|J|} \,, \tag{7}$$

one comes to

$$\cos\varphi = \frac{\beta}{2(1-\alpha)} \,, \tag{8}$$

$$W_2 = -\frac{\tilde{z}|J|N}{2}\left[1 + \frac{\beta^2}{2(1-\alpha)}\right]. \tag{9}$$

A comparison of W_1 and W_2 gives the value of magnetic field induction corresponding to the first-order bulk spin-flop transition from the collinear phase to the spin-flop phase:

$$\beta_1 = 2\sqrt{\alpha(1-\alpha)} \approx 2\sqrt{\alpha}\,. \tag{10}$$

Angle φ for $\beta > \beta_1$ decreases as the field grows, and at $\beta = \beta_2$, with

$$\beta_2 = 2(1-\alpha)\,, \tag{11}$$

sublattices collapse, i.e., angle φ vanishes. This second-order phase transition is called the spin-flip transition. For $\beta > \beta_2$, magnetizations of antiferromagnet sublattices are parallel, and we shall refer to this phase as ferromagnetic.

Let us move to a consideration of the surface spin-flop transition starting from an atomically smooth surface. Sections through the antiferromagnet surface relate to two classes. Compensated sections correspond to a case in which atomic planes parallel to the surface contain an equal number of atoms belonging to different sublattices. The magnetic moment of such planes in the collinear phase is zero.

Uncompensated sections correspond to a case in which atomic planes parallel to the surface contain atoms of a single sublattice, while the adjoining atomic planes consist of atoms belonging to different sublattices and have opposite magnetic moments in the collinear phase.

In the case of a compensated section, there is no surface phase transition, and spins of the atomic surface layer undergo flop in the bulk spin-flop transition field β_1. This phenomenon is attributable to the atomic scale of the change in the antiferromagnetic order parameter equaling the difference between sublattice magnetization vectors and the energetic inefficiency of such distortions [2].

In what follows, we shall consider uncompensated sections alone. The surface spin-flop transition for this case was investigated for the first time in Ref. [3], where it was shown that the surface magnon dispersion law is softened at

$$\beta_s = \frac{\beta_1}{\sqrt{2}} \,. \tag{12}$$

Later authors [4, 5] studied the distribution of the antiferromagnetic order parameter in a field range of $\beta_s < \beta < \beta_1$ based on the assumption that bulk spin-flop orientation occurring for $\beta > \beta_1$ is realized at the antiferromagnet surface; i.e., the antiferromagnetic vector in the atomic surface layer is normal to the easy axis.

The bulk of an antiferromagnet for $\beta < \beta_1$ being in the collinear phase, a 90° exchange spring must form near its surface, the structure of which coincides with that of the Bloch domain wall.

The hypothesis of spin-flop orientation at the antiferromagnetic surface is redundant because spin distribution can be found without additional assumptions. Moreover, it was shown in Ref. [2] that such conjecture is erroneous because a 180° exchange spring rather than the 90° one forms near the surface.

The surface spin-flop transition has not been a focus for researchers for many years since the publication of Refs [4, 5]. A new impetus to investigations was given by the discovery of giant magnetoresistance in multilayer magnetic structures (see, for instance, works [6–8]), demonstrating that the behavior of such structures with alternating ferromagnetic and nonmagnetic layers a nanometer thick and with the antiferromagnetic exchange sign between adjacent ferromagnetic layers in a magnetic field is, in many respects, analogous to the behavior of the plane-parallel layer of an antiferromagnet having uncompensated surfaces.

The review outline is as follows. Section 2 deals with surface phase transition in a semi-infinite antiferromagnet with an uncompensated surface. Size effects in the plane-parallel layer of an antiferromagnet are described in Section 3, with special reference to the essential difference between the behavior of layers containing an even and odd

number of atomic planes. Section 4 is devoted to the study of spin-flop transition at the rough uncompensated surface of a semi-infinite antiferromagnet. Section 5 describes a phase diagram of the plane-parallel layer of an antiferromagnet with uncompensated rough surfaces. The closing Section 6 is a synopsis of reviewed issues.

2. Smooth surface of a semi-infinite specimen

Because the number of nearest neighbors for spins located at the antiferromagnet surface is smaller than in the bulk, they are more amenable to the exposure to an external magnetic field. It is this fact that explains why the field of spin-flop transition is smaller than its bulk value.

Let us assume that the easy axis lies in the surface plane and label the uncompensated atomic planes parallel to the surface with the index j starting from the surface. Even and odd j values correspond to different sublattices. The location of the spins in the atomic plane is given by angle θ_j between the easy axis and the spin magnetic moment. Atomic magnetic moments are supposed to be confined to the respective atomic plane. Then, the surface magnetic moment resulting from spin-flop transition has no constituent perpendicular to the surface. Otherwise, a magnetic field arises that causes the system's energy to increase.

With this assumption in mind, the energy of exchange interaction can be expressed as

$$W_{\mathrm{ex}} = \frac{n|J|\tilde{z}}{4} \sum_{j=1}^{\infty} \left[\cos(\theta_j - \theta_{j-1})(1 - \delta_{1,j}) + \cos(\theta_j - \theta_{j+1})\right], \tag{13}$$

where n is the number of spins in the atomic plane, and $\delta_{i,j}$ is the Kronecker symbol. The number of nearest neighbors of a given spin in preceding or subsequent atomic planes is $\tilde{z}/2$. For section (100) across a tetragonal body-centered lattice (with easy axis c lying in the section plane), one finds $\tilde{z} = 8$.

For the energy of single-ion anisotropy and Zeeman energy we obtain the following formulas

$$W_{\mathrm{an}} = -Kn \sum_{j=1}^{\infty} \cos^2\theta_j, \tag{14}$$

$$W_B = -\mu B_0 n \sum_{j=1}^{\infty} \cos\theta_j, \tag{15}$$

with the magnetic field applied parallel to the easy axis.

Minimization of the total energy W over parameters θ_j yields the system of equations

$$\sin(\theta_j - \theta_{j-1})(1 - \delta_{1,j}) + \sin(\theta_j - \theta_{j+1}) = 2\alpha \sin 2\theta_j + 2\beta \sin\theta_j. \tag{16}$$

This system was solved in Ref. [2] by numerical methods.

It turned out that if the magnetic moment of the upper atomic plane in a weak magnetic field is antiparallel to it ($\theta_1 = \pi$), then surface spin-flop transition occurs in field β_{s}, giving rise to a 180° exchange spring near the surface: magnetization of the upper atomic plane turns in the field direction, while magnetizations of the second and third, fourth and fifth, etc. atomic planes are pairwise compensated. The magnetization of the first atomic plane being parallel to that of the last even atomic plane, the spin-flop transition near the antiferromagnet surface results in the appearance of a magnetic moment equal to $2\mu n$ [2]. It is possible to observe a 180° turn of the upper atomic plane magnetization vector by magnetic force, spin-polarized tunnel, and photoemission electron microscopies.

The characteristic scale at which the rotation of atomic plane magnetizations takes place in the exchange spring of interest can be estimated from the asymptotic behavior of angles θ_j.

In the depth of an antiferromagnet, the values of θ_j are slightly different from the bulk values (0 for even and π for odd planes). This allows system (16) to be linearized with respect to these deviations [2]:

$$\chi_{2n} = \theta_{2n}, \qquad \chi_{2n-1} = \theta_{2n-1} - \pi.$$

The linearized equation has the following solution

$$\chi_n = \kappa \chi_{n-1}, \tag{17}$$

where

$$\kappa = 1 - \sqrt{\beta_1^2 - \beta^2}, \tag{18}$$

corresponding to the exponential decrease in distortions toward the depth of the antiferromagnet:

$$\chi_n = \chi_1 \exp\left[-\frac{d(n-1)}{r_{\mathrm{c}}}\right], \tag{19}$$

where d is the distance between the nearest atomic planes, and r_{c} is the correlation radius of the order parameter:

$$r_{\mathrm{c}} = \frac{d}{|\ln|\kappa||} = \frac{d}{\sqrt{\beta_1^2 - \beta^2}} \propto (\beta_1 - \beta)^{-1/2}. \tag{20}$$

Such dependence of the correlation radius for $\beta < \beta_1$ was first obtained in Ref. [5]. Evidently, as $\beta \to \beta_1$, r_{c} tends to infinity as $(\beta_1 - \beta)^{-1/2}$, i.e., the surface spin-flop transition spreads deep into the antiferromagnet as it approaches the bulk spin-flop transition point.

For $\beta > \beta_1$, i.e., after the bulk spin-flop transition has already occurred, it is energetically preferred for the magnetization of the upper (first) atomic plane to be directed along the field; therefore, the 180° spiral turns into a 90° one: the antiferromagnetic vector is perpendicular to the easy axis in the bulk, and collinear to it near the surface. A flop of sublattices in the near-surface layer occurs in stronger magnetic fields ($\beta \sim 0.25$).

If the magnetic moment of the upper atomic plane in weak magnetic fields is parallel to the field vector ($\theta_1 = 0$), the surface spin-flop transition is energetically unfavorable and the bulk transition occurs at $\beta = \beta_1$.

The situation for $\beta > \beta_1$ is totally analogous to the case of $\theta_1 = \pi$, the sole difference being in the direction of rotation of the antiferromagnetic order parameter within the exchange spring.

The characteristic scale of the exchange spring can also be found from the asymptotic behavior of angles θ_j. In this case, however, deviations of angles θ_j from their bulk values in the spin-flop phase, viz. $\chi_{2n-1} = \theta_{2n-1} - \varphi$ and $\chi_{2n} = \theta_{2n} + \varphi$, are small [$\varphi$ is given by formula (8)].

The solution of the linearized equation has the form (19), where, according to Ref. [2], one finds

$$\kappa = 1 - \sqrt{\beta^2 - \beta_1^2}. \tag{21}$$

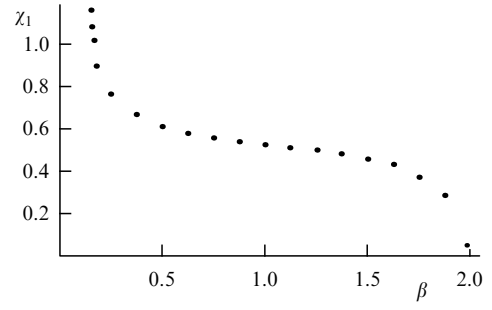

Figure 2. Rotation angle of the magnetic moment of the surface atomic layer versus magnetic field stronger than the bulk spin-flop transition field for $\alpha = 0.005$.

As β grows in the region of $\beta > \beta_1$, the exchange spring near the surface does not disappear, but the angle of turn in it decreases. The dependence of $\chi_1 = \theta_1 - \varphi$ on the magnetic field induction is shown in Fig. 2.

Moreover, the spiral shrinks due to decreasing the correlation radius r_c. Parameter κ, describing asymptotic behavior of deviations χ_j within the field range $\beta_1 \ll \beta < \beta_2$, is given by the expression [2]

$$\kappa = 1 + \frac{2\beta^2}{\beta_2^2 - 2\beta^2} \pm \sqrt{\left(1 + \frac{2\beta^2}{\beta_2^2 - 2\beta^2}\right)^2 - 1}\,. \qquad (22)$$

It is easy to see that $\kappa \to 0$ as $\beta \to \beta^* = \beta_2/\sqrt{2}$, and the correlation radius also vanishes. This situation corresponds to that at $\beta = \beta^*$ when only angle θ_1 determining the magnetization direction in the upper atomic plane undergoes deviation from the bulk value. The sign of this deviation is such that magnetization makes an angle with the magnetic field vector smaller than in the crystal bulk.

At $\beta = \beta^*$, the sign of κ changes. If $\beta < \beta^*$, the parameter $\kappa > 0$ [a minus sign in formula (22)], while for $\beta > \beta^*$ this parameter is negative [a plus sign in formula (22)].

As the magnetic field grows within the $\beta^* < \beta < \beta_2$ range, the characteristic size of the exchange spring increases and tends to infinity as $(\beta_2 - \beta)^{-1/2}$ when $\beta \to \beta_2 - 0$. Because all angles θ_j and χ_j in the limit $\beta \to \beta_2$ tend to vanish, the solution of system (16) can be found analytically [2].

Let us introduce a dimensionless parameter

$$\Delta = 1 - \frac{\beta}{\beta_2}\,. \qquad (23)$$

It follows from formula (8) that

$$\varphi = \sqrt{2\Delta}\,. \qquad (24)$$

Using expression (22), we obtain

$$\kappa = \sqrt{8\Delta} - 1\,.$$

The linearized equation for χ_1 yields

$$\chi_1 = \sqrt{2\Delta}\left(\sqrt{2\Delta} - 1\right). \qquad (25)$$

Then, we arrive at

$$\theta_1 = 2\Delta\,. \qquad (26)$$

Thus, the values of angle φ in the bulk as $\beta \to \beta_2$ differ from zero by approximately $\sqrt{\Delta}$, whereas the value of θ at the surface is on the order of Δ as expected because the magnetic moment of the upper atomic plane makes an angle with the magnetic field direction smaller than the respective angle in the bulk.

The correlation angle $r_c = d/\sqrt{8\Delta} \propto \Delta^{-1/2}$, in conformity with the mean field theory for second-order phase transitions.

It can be concluded that distortions of the antiferromagnetic order parameter (supplemental to those in the bulk) caused by a magnetic field near the uncompensated antiferromagnetic surface emerge in the field β_s of surface spin-flop transition and persist as the field grows to a value corresponding to the spin-flip transition to the ferromagnetic phase.

3. Size effects in the plane-parallel layer of an antiferromagnet with smooth uncompensated surfaces

For $\alpha \ll 1$, in the case of uncompensated antiferromagnet surface, the order parameter correlation radius r_c in fields $\beta \sim \beta_1$ is much larger than the interatomic distance; for this reason, both in this field range and near the value of the spin-flip transition field at which r_c becomes comparable to or greater than the antiferromagnetic layer thickness, marked size effects are likely to arise.

As mentioned in Section 2, a system comprising alternating ferromagnetic and nonmagnetic metallic layers with the antiferromagnetic sign of exchange between the nearest ferromagnetic layers behaves in the magnetic field like the antiferromagnetic layer under consideration.

Theoretical studies of such multilayer structures have been undertaken using numerical methods by many authors [9–16], whereas attempts at analytical consideration of size effects are virtually absent.

A recent publication [17] reports on the investigation of the ground state of an antiferromagnetic atomic chain on a ferromagnetic substrate by numerical methods. The main simplification made in work [17] reduces to the fact that the spins of the ferromagnet are taken as unperturbed by interaction with the chain. This assumption is valid provided the energy of exchange interaction between the neighboring spins in the ferromagnet is much higher than that of the interaction between the spins of the substrate and the chain. In this case, the exchange field created by the ferromagnetic substrate plays the role of the external field for the antiferromagnetic chain, and the problem of chain spin behavior as shown in Ref. [18] reduces to the problem of spin-flop and spin-flip transitions in the thin antiferromagnetic layer considered in Ref. [19].

Changes in formulas (13)–(16) for the description of an antiferromagnet of finite thickness are reduced to the number of terms in the sum over j also being finite and equaling the number M of atomic planes in the layer, while term $\cos(\theta_j - \theta_{j+1})$ on the right-hand side of Eqn (13) and term $\sin(\theta_j - \theta_{j+1})$ on the left-hand side of Eqn (16) must be multiplied by $(1 - \delta_{M,j})$.

As shown in paper [19], layers containing even and odd number of atomic planes behave quite differently. Such a difference for multilayer structures with $M = 15$ and $M = 16$ was first described in Ref. [9]).

Even M. In this layer, surface atomic planes belong to different sublattices of the antiferromagnet. In magnetic fields $\beta < \beta_s$, the layer is in the collinear phase. Spin-flop transition in this layer occurs at $\beta = \beta_s$ and results in

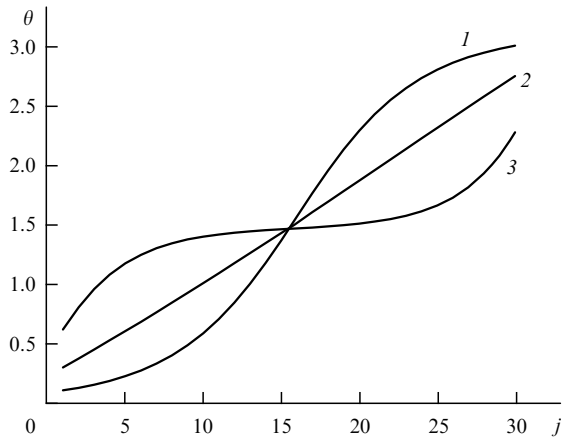

Figure 3. Domain walls in a layer with an even number of atomic planes in fields $\beta_s < \beta < \beta_1$ (curve *1*), $\beta \approx \beta_1$ (curve *2*), and $\beta > \beta_1$ (curve *3*). The dependence of the turn angle of the antiferromagnetism vector on the atomic plane number is depicted.

appearing a 180° Bloch domain wall in its center [9, 19]. The wall occupies only the middle part of the layer if correlation radius $r_c(\beta_s)$ given by formula (20) is smaller than the layer thickness a (curve *1* in Fig. 3). The appearance of the wall accounts for the magnetic moments of surface atomic planes being directed along the magnetic field vector.

If the layer thickness $a < r_s \equiv r_c(\beta_s) = d\beta_s^{-1} \approx d/\sqrt{2\alpha}$, the layer accommodates only the central part of the domain wall in which the rotation angle of the antiferromagnetic vector changes linearly with distance.

As the effective field grows and β approaches β_1, the correlation radius tends to infinity as $(\beta_1 - \beta)^{-1/2}$. When $a \gg r_s$, the domain wall broadens and extends over the entire layer thickness in field β_a, which can be found from the condition

$$2r_c(\beta_a) \approx a\,. \tag{27}$$

As r_c grows further, the thickness of the domain wall ceases to increase, and the antiferromagnetism vector turns uniformly through angle π from one layer surface to the other, so that magnetizations of extreme atomic planes are directed along the external field vector (straight line *2* in Fig. 3).

Radius r_c in exchange fields stronger than β_1 begins to decrease and the 180° domain wall in the layer center transforms into two roughly 90° exchange springs near the surfaces (curve *3* in Fig. 3).

Then, the middle of the layer is in the spin-flop phase. r_c decreases with growing field, size effects become immaterial, and the behavior of the exchange spring near one of the layer surfaces is described irrespective of the other's behavior. Characteristics of this behavior were considered in Section 2.

The correlation radius r_c increases as the field approaches the value of the bulk spin-flip transition field β_2 and the size effect again becomes essential.

Simulation in work [19] demonstrated that spin-flip transition in a layer of finite thickness is actually a second-order phase transition and occurs in field $\beta_2^* < \beta_2$ (Fig. 4).

The dependence thus obtained can be approximated by the formula

$$\beta_2^* = \beta_2\left[1 - \frac{1}{8}\left(\frac{4.5}{M}\right)^2\right]. \tag{28}$$

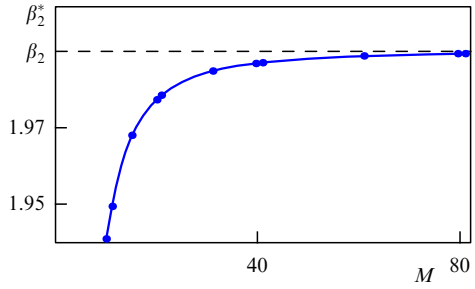

Figure 4. Plot of the spin-flip transition field vs. the number of atomic planes in the layer.

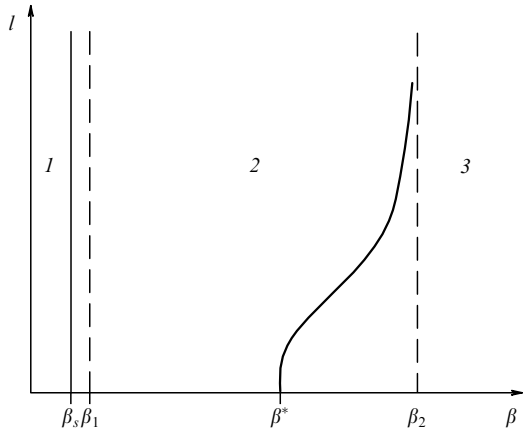

Figure 5. 'Magnetic field–layer thickness' phase diagram for a layer with an even number of atomic planes: collinear antiferromagnetic phase (*1*), noncollinear phase (*2*), and ferromagnetic phase (*3*). Solid curves correspond to phase transition lines.

The phase diagram of a layer with an even number of atomic planes in 'magnetic field–layer thickness' variables is presented in Fig. 5.

Odd M. In this layer, both surface atomic planes belong to the same sublattice of the antiferromagnet. We assume that the total magnetic moment, and hence magnetic moments of surface planes, are directed along the external magnetic field vector.

As shown in Section 2, spin-flop transition in the surface layer in this configuration is suppressed. Therefore, spin-flop transition in a layer of finite thickness occurs for $\beta_1^* > \beta_1$; furthermore, it is a second-order phase transition unlike transitions in an infinite specimen or in a layer with an even number of atomic planes [19]. The magnetization rotation angle changes continuously following field variation, with its maximum being located in the center of the layer (see Figs 6 and 7).

Theoretical dependence $\beta_1^*(M)$ plotted in Fig. 8 is approximated by the expression

$$(\beta_1^*)^2 = \beta_1^2 + \left(\frac{4}{M}\right)^2. \tag{29}$$

The behavior of a layer with odd M for $\beta > \beta_1^*$ is similar to that in the case of even M.

The phase diagram of a layer with an odd number of atomic planes is shown in Fig. 9.

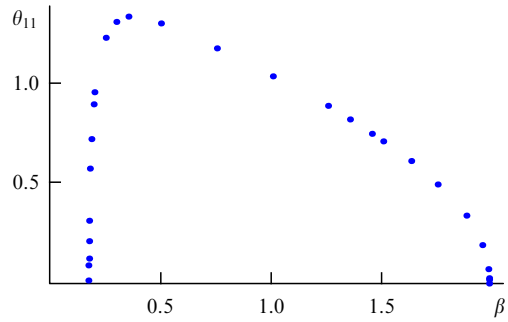

Figure 6. Magnetic field dependence of the direction of the magnetization vector in the middle atomic plane for a layer with $M = 21$ at $\alpha = 0.005$.

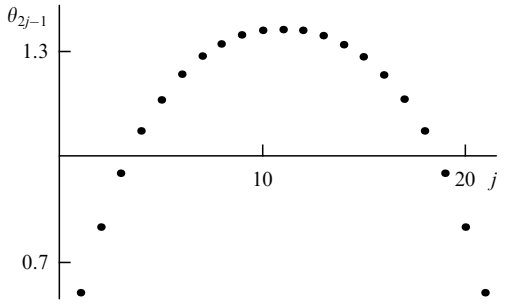

Figure 7. Direction of magnetization vectors of odd atomic planes in field $\beta = 0.2$ for a layer with $M = 41$ at $\alpha = 0.005$.

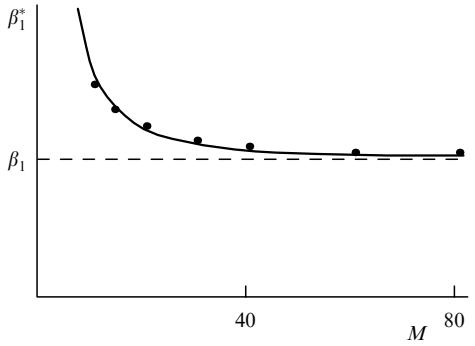

Figure 8. Plot of spin-flop transition field vs. the number of atomic planes in a layer with an odd number of atomic planes.

Thus, the character of spin-flop transition depends on the parity of the number of atomic planes in the layer. At even M, spin-flop transition is a first-order phase transition and always occurs in the surface spin-flop transition field. At odd M, a second-order phase transition takes place in the M-dependent field stronger than the bulk spin-flop transition field.

Spin-flip transition in a layer of finite thickness occurs in a field weaker than the bulk spin-flip transition field.

4. A semi-infinite antiferromagnet with an uncompensated rough surface

The rough surface of an antiferromagnet has atomic steps as high as one atomic layer. The upper atomic layer at either side of the step belongs to different sublattices of the antiferromagnet (Fig. 10). Due to this, the entire antiferromagnet

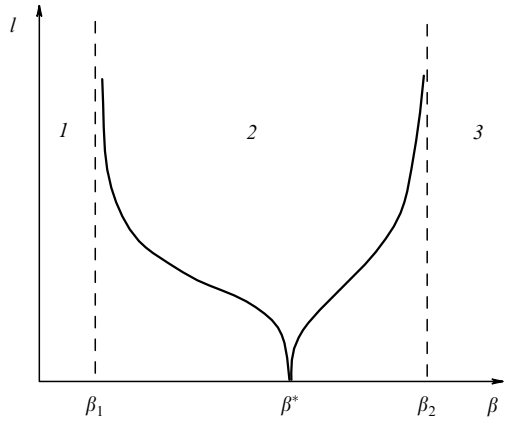

Figure 9. 'Magnetic field–layer thickness' phase diagram for a layer with an odd number of atomic planes: collinear antiferromagnetic phase (*1*), noncollinear phase (*2*), and ferromagnetic phase (*3*). Solid curves correspond to phase transition lines.

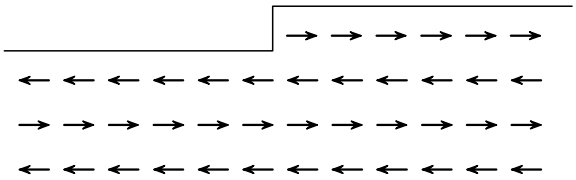

Figure 10. Atomic step at the surface of an antiferromagnet. Arrows show directions of atomic spins.

surface is broken up by step edges into type 1 and 2 regions, the type being determined by the number of the sublattice to which the upper atomic layer belongs.

Given the sufficiently large characteristic longitudinal size of the steps, R, application of magnetic field β satisfying inequality $\beta_s < \beta < \beta_1$ parallel to magnetization of the first sublattice does not change the magnetic structure of type 1 regions, whereas surface spin-flop transition occurs in type 2 regions. As a result, the surface is broken down into domains.

The nature of surface distortions of the magnetic structure strongly depends on the relationship between characteristic step width R and the correlation radius of the order parameter r_c. The strong dependence of r_c on β, in particular, the tendency of r_c to infinity as $\beta \to \beta_1$, accounts for a sufficiently complicated phase diagram of magnetic structure distortions in variables (β, R). It was examined in Ref. [20] for the example of tetragonal body-centered lattice of spins whose direction was given by unit vector $\mathbf{s}_{n,i,j}$, where index n labelled planes beginning from the uppermost one of those present in a sample with a rough surface, while indices i and j gave spin positions in the plane where they formed a rectangular lattice. The spin value was regarded to be constant and included in the corresponding interaction constants.

The Heisenberg exchange interaction described in the nearest neighbor approximation by the expression

$$W_{ex} = \frac{|J|}{2} \sum_{n,i,j,\delta} (\mathbf{s}_{n,i,j},\ \mathbf{s}_{(n,i,j)+\delta}) , \qquad (30)$$

where index δ labels the nearest neighbors of a given spin, was taken into account during computations, along with the

uniaxial anisotropy energy in the form

$$W_M = K_\perp \sum_{n,i,j} (s^z_{n,i,j})^2 - K \sum_{n,i,j} (s^x_{n,i,j})^2 , \tag{31}$$

where the z-axis of the orthogonal Cartesian system of coordinates is normal to the surface, and the x-axis parallel to the surface is the easy axis. The surface anisotropy constant $K_\perp$ is introduced to take into account the energetic inefficiency of states in which the arising magnetic moment has a z-component perpendicular to the surface. For $K_\perp > 0$, spins lie in atomic planes parallel to the surface and their direction is given by angle $\theta_{n,i,j}$ which makes an easy axis with the magnetic moment corresponding to the spin. Direct account of dipole–dipole interaction between spins and arising demagnetizing fields considerably complicates the problem and increases computation time.

The Zeeman energy assumes the form

$$W_Z = \mu \sum_{n,i,j} (\mathbf{s}_{n,i,j}, \mathbf{B}_0) . \tag{32}$$

This expression takes into account that the spin vector is antiparallel to the vector of the magnetic moment corresponding to the spin. Equilibrium spin distribution was found by simulation of spin behavior based on the system of Landau–Lifshitz–Hilbert equations

$$\hbar S_{af} \frac{d}{dt} \mathbf{s}_{n,i,j} = [\mathbf{s}_{n,i,j}, \mathbf{H}_{eff}] + \gamma \mathbf{H}_{eff} , \tag{33}$$

where γ is the attenuation coefficient, and S_{af} is the atomic spin, and

$$H^p_{eff} = -\frac{\partial W}{\partial s^p_{n,i,j}} , \tag{34}$$

$p = x, y, z$, and W is the total energy: $W = W_{ex} + W_{an} + W_Z$.

The initial state was chosen as either the collinear state of the antiferromagnet, corresponding to the minimal energy in the absence of the external field, or the homogeneous state developing after bulk spin-flop transition. The solution of the system (33) was sought by the 'classical' fourth-order Runge–Kutta method. Arrival at equilibrium was established from the behavior of the total energy of the system.

Simulation was performed for the case in which step edges were parallel to the y-axis of the orthogonal system of coordinates; in other words, the two-dimensional problem with boundary conditions periodic in x was being solved. This limitation did not qualitatively change the generality of the results. They suggest formation of a near-surface 180° exchange spring in the surface spin-flop transition field of type 2 regions where the magnetic moment of the surface atomic layer in weak fields is antiparallel to the external magnetic field; these results were obtained under conditions in which the characteristic size R of steps was much bigger than the correlation radius r_c of antiferromagnetic order parameter (Fig. 11).

As R decreases but remains larger than r_s, the spin-flop transition field in a bounded type 2 region shifts toward stronger magnetic fields (Fig. 12). For $R < r_s$, no domain wall whatever forms in a separate region.

As the external field approaches the bulk spin-flop transition point β_1, the correlation radius $r_c \to \infty$; therefore, relation $R > r_c$ breaks down with the growth of the magnetic

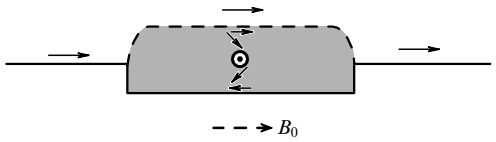

Figure 11. Exchange spring in the type 2 region. Solid arrows indicate the local direction of the antiferromagnetism vector whose rotation occurs in the plane parallel to the surface. Dashed arrow points to the direction of the magnetic field.

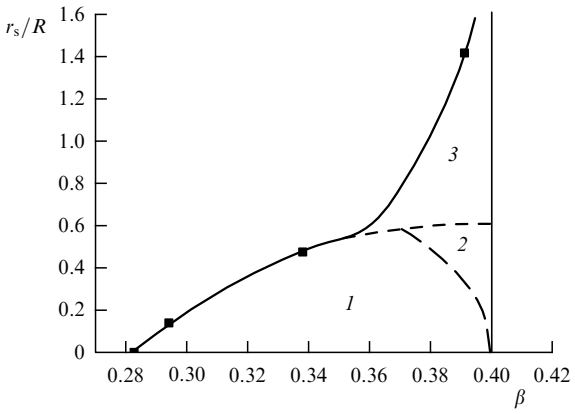

Figure 12. 'Magnetic field–roughness' phase diagram in the field range $\beta \leqslant \beta_1$ for $\alpha = 0.04$. Solid curve is the line of first-order phase transitions from the collinear to noncollinear phase. Domain (*1*), vortex (*2*), and weak distortion (*3*) regions are shown.

field even if the domain phase emerges. As shown in paper [20] for the field range in which $r_c \gg R$, the problem in question reduces to that of the distortion of order parameters at the rough interface in a two-layer ferromagnet–antiferromagnet system [21, 22] provided the ferromagnet is absolutely rigid against magnetic distortions and interlayer exchange is substituted by magnetic field β.

Calculations suggest the formation of static spin vortices near the antiferromagnetic surface, spreading over the region with $|z| < R$; their boundaries at this surface coincide with atomic step edges. There appears another characteristic size δ_0, besides R; it is the width of the surface region near an atomic step in which $\theta_{n,i,j}$ is essentially different from its optimal value (0 and π on either side of the step, respectively).

Let us estimate δ_0 for the case of $R \gg \delta_0$ on energetic grounds. The fact that magnetization of the upper atomic layer in the region of width δ_0 does not coincide with magnetic field direction accounts for the loss of Zeeman energy (expressed hereinafter in $\tilde{z}|J|$ units) on the order of $\beta\delta_0/S_0$ per unit length of the atomic step, where S_0 is the area of a rectangular cell in the atomic plane. The loss of anisotropy energy $\alpha\delta_0/S_0$ is negligibly small compared with that of Zeeman energy.

Within the range of $\delta_0 < \rho < R$, where ρ is the shortest distance from a point to the step edge at the antiferromagnet surface, $|\nabla\theta|$ is inversely proportional to ρ. In this range, the contribution of distortions of the antiferromagnetic order parameter to the exchange energy per unit length of the atomic step is on the order of $b_y^{-1} \ln(R/\delta_0)$, where b_y is the parameter of crystal lattice along the atomic step edge [21, 22]. Minimization of the total energy over δ_0 leads to $\delta_0 \sim b_x/\beta$

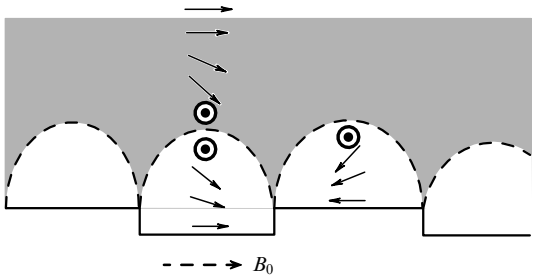

Figure 13. Static spin vortices and the 90° exchange spring. The region where the spring exists is shown in dark grey. Solid arrows indicate the local direction of the antiferromagnetism vector rotating in the plane parallel to the surface. The dashed arrow points to the direction of the magnetic field.

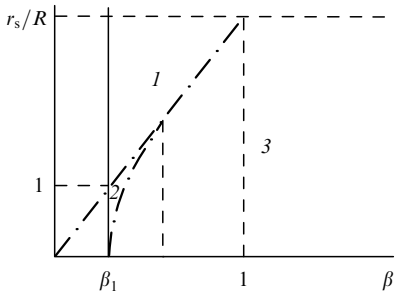

Figure 14. 'Magnetic field-roughness' phase diagram in the field region of $\beta > \beta_1$. Weak distortion (*1*), vortex (*2*), and domain (*3*) existence regions are shown.

(where b_x is the crystal lattice parameter along the x-axis); in the $\beta \sim \beta_1$ range, the value of δ_0 is of order r_s.

In the opposite case of $R \ll \delta_0$, magnetization has no space to turn. This is the weak distortion region.

As mentioned earlier, atomic steps break up the entire antiferromagnet surface into regions of two types having total areas σ_1 and σ_2, respectively. If the mean value of θ in the range of $R \ll |z| \ll r_c$ is ψ, then θ changes from zero to ψ in vortices occupying type 1 regions and from ψ to π in vortices of type 2 regions.

The total vortex energy can be written out by analogy with that in Slonczewski's 'magnetic proximity' model [23] as

$$W = C_1\psi^2 + C_2(\pi - \psi)^2 , \tag{35}$$

where

$$C_k = \frac{\sigma_k}{R} . \tag{36}$$

In the case of $\sigma_1 = \sigma_2$, the vortex energy minimum corresponds to $\psi = \pi/2$.

Thus, formation of a 90° exchange spring near the antiferromagnet surface is needed to decrease the vortex energy (Fig. 13). An additional surface energy

$$w \sim \sqrt{\beta_1^2 - \beta^2} \tag{37}$$

is associated with the appearance of the spring; it vanishes as $\beta \to \beta_1$. In the field range under consideration, when $\delta_0 \ll R \ll r_c$, the newly formed exchange spring accounts for the much higher gain in the vortex energy compared with its loss.

For $r_s \ll R$, domain–vortex phase transition occurs continuously in the field β_R for which $r_c(\beta_R) \sim R$, i.e., at

$$\tau_R \equiv 1 - \frac{\beta_R}{\beta_1} \sim \frac{r_s^2}{R^2} . \tag{38}$$

The magnetic field–roughness phase diagram for $\beta < \beta_1$ is depicted in Fig. 12.

For $R \ll r_s$, a phase transition from the collinear state occurs directly to the phase with weak distortions.

Simulation in the framework of a discrete model demonstrated that the transition from the collinear phase to the phase with weak distortions and 90° exchange spring is a first-order surface phase transition in the field $\tilde{\beta}_R$, the value of which can be estimated from simple energetic reasoning [20]:

$$\tilde{\tau}_R \equiv 1 - \frac{\tilde{\beta}_R}{\beta_1} \sim \left(\frac{R}{r_s}\right)^2 \ll 1 . \tag{39}$$

After the bulk spin-flop transition has already occurred in the field range $\beta > \beta_1$, the behavior of surface distortions is virtually identical at all R. Because $r_c \to \infty$ as $\beta \to \beta_1 + 0$, the system near the field value β_1 is in the vortex phase or in the phase of weak distortions, while surface distortions penetrate inside the antiferromagnet to the depth of order R. In the case of $\sigma_2 = \sigma_1$, the bulk spin-flop transition results in elimination of the exchange spring.

As the field grows, r_c decreases as described by formula (21), and δ_0 changes as β^{-1}. At the values of $\beta \geqslant 1$ rather far from the value of sublattice collapse field β_2, the parameters r_c and δ_0 are of the same order comparable to the lattice constant.

In the field β'_R with $r_c(\beta'_R) = R \gg \delta_0(\beta'_R)$, a smooth transition occurs to the domain phase where in the regions of either type roughly 90° exchange springs form with an oppositely rotating antiferromagnetic order parameter (from $\theta = 0$ at the surface to $\theta = 90°$ in the bulk in the type 1 region, and from $\theta = 180°$ at the surface to $\theta = 90°$ in the bulk in the type 2 region). For β'_R, the following estimate is valid:

$$\tau'_R = \frac{\beta'_R}{\beta_1} - 1 \sim \frac{r_s^2}{R^2} . \tag{40}$$

As the field grows, rotation of magnetization of the upper atomic layer deflects it from the magnetic field direction and approaches the magnetization direction of the respective sublattice in the bulk. The angle of rotation in the exchange spring gets smaller, and its thickness decreases as the field grows up to the value of $\beta^* = \beta_2/\sqrt{2}$.

For $\beta_2 > \beta > \beta^*$, rotation of the antiferromagnetic order parameter in regions of either type, unlike that in the field range $\beta_1 < \beta < \beta^*$, has only one sign; due to this, the difference between the regions becomes insignificant and further evolution of surface distortions proceeds similarly to their evolvement in the case of smooth surfaces considered in Section 2.

Only weak surface distortions are apparent when $R < \delta_0(\beta)$. The phase diagram for the field range $\beta_2 > \beta > \beta_1$ is presented in Fig. 14.

Now, let us consider the possibility of observing these distortions in experiment. The positions of atomic step edges at the antiferromagnet surface and the characteristic distance between them can be found using atomic-force microscopy.

Unfortunately, parameter R is not prominent enough under experimental conditions and only root-mean-square deviation of the surface from its average position is usually estimated. Indirect estimation gives the values from 1 to 10 nm for R. Improved crystal and nanolayer growth technologies make it possible to decrease the concentration of atomic steps and increase R. In weak magnetic fields, the upper atomic planes on either side of an atomic step in the collinear phase are magnetized in opposite directions, as can be shown by magnetic microscopy. In the domain phase, magnetizations of the upper atomic plane have identical orientation in regions of both types. Due to this, the field of spin-flop transition in type 2 regions can be found experimentally. Magnetic microscopy can identify boundaries between the regions and shows that they coincide with atomic step edges. The magnetization direction at the boundaries differs from that in the center of the regions; in particular, at the center of the transition region it is normal to the easy axis. The width δ_0 of the transition region varies from 10 to 100 nm, depending on the degree of anisotropy, and for $\beta \leqslant \beta_1$ is of the same order of magnitude as the width of the domain wall in the absence of a magnetic field.

The phase with weak distortions is easy to identify based on the deflection of the mean magnetization of the surface atomic layer from the direction of the magnetic field and easy magnetization axis. In fields $\beta > \beta_1$, it is possible to observe a transition from the phase with weak distortions to the vortex or domain phase.

5. An antiferromagnetic layer with uncompensated rough surfaces

Antiferromagnetic layers a nanometer thick find wide application in modern magnetoelectronics. Hence, there is great interest in the investigation of their properties.

The antiferromagnetic layer can be mentally divided into regions whose boundaries are perpendicular to the layer plane. The boundary plane passes across the atomic step edge on one of the layer surfaces. The behavior of magnetization in each region depends on the number of atomic planes belonging to each of the two sublattices of the antiferromagnet. This number is constant within the region. The type of the region is determined by a combination of two parameters: parity (or nonparity) of the number of atomic planes [even (E) or odd (O)], and the number of the antiferromagnetic sublattice to which the upper atomic plane (A or B) belongs. A total of four combinations are conceivable, giving rise to four region types (EA, EB, OA, OB).

As shown in Section 3, the character of a spin-flop transition in the case of a layer with smooth boundaries strongly depends on the parity of the number of atomic planes:

- a first-order spin-flop transition in a layer with an even number of atomic planes occurs in the surface spin-flop transition field. It results in a state with the domain wall centered in the middle of the layer;
- a second-order spin-flop transition in a layer with an odd number of atomic planes occurs in a field stronger than the bulk spin-flop transition field and dependent on the layer thickness.

Given the sufficiently large distance R between steps, the antiferromagnetic layer in a magnetic field is broken into domains whose boundaries coincide with region boundaries, i.e., are perpendicular to the layer plane and intersect the edge of an atomic step on one of its surfaces. The magnetization behavior in each domain is dictated by the type of the respective region.

Magnetic structure distortions within the entire range of variations of magnetic fields and R values were studied in the framework of the model described in Section 4 in Ref. [24].

The chosen layer was cut out perpendicular to the direction [100] of the tetragonal body-centered lattice. The behavior of thin ($a \ll r_s$) and thick ($a \gg r_s$) antiferromagnetic layers in the magnetic field $\beta \leqslant \beta_1$ proved significantly different. Therefore, these cases are described separately below.

5.1 The thin layer

5.1.1 $R \gg r_s$. We shall consider the spin distribution in regions of all types on the assumption that the region size R is larger than other characteristic lengths of the problem.

OA and OB regions possess a magnetic moment equal to that of a single uncompensated atomic plane. Therefore, a second-order spin-flop transition in the OA region occurs in the field β_1^* [see formula (29)]. In the case of a thin layer, formula (29) takes the form

$$\beta_1^* \approx \frac{4}{M} \approx \frac{4\beta_s r_s}{a} \gg \beta_1 . \tag{41}$$

Upon field switching-on, the magnetic moment in the OB region is directed against the field. In the OB type layer with smooth boundaries, a change in direction of the antiferromagnetism vector to the opposite one occurs in an arbitrary weak field. For this reason, such initial orientation was not considered in Section 3. Reorientation of the antiferromagnetism vector in a region of finite dimension is accompanied by a substitution of the OA type for the OB one and the appearance of a 180° domain wall along its perimeter, which is perpendicular to the layer surface.

The characteristic field of this phase transition can be found by equating the gain in the Zeeman energy to the energy of the newly formed domain wall. The gain is on the order of β per cell in the layer plane (expressed hereinafter in $\tilde{z}|J|$ units). The surface energy of the domain wall in the antiferromagnet is on the order of $\sqrt{\alpha}$ per elementary cell area, and the wall thickness is on the order of r_s. The area of the region on the layer surface being $\sim R^2$, and that of the domain wall $\sim Ra$, the characteristic reorientation field is defined as

$$\beta_{reor} \approx \frac{a\sqrt{\alpha}}{R} \approx \frac{a}{R}\,\beta_1 \ll \beta_1 . \tag{42}$$

As shown below, the arising domain wall is practically totally confined to the region with an even number of atomic planes because its formation in such a region is unaccompanied by an appreciable increase in the Zeeman energy.

Domain walls perpendicular to the layer are described in the continual approximation.

Let us carry out the change of variables $\tilde{\theta}_{2n-1,i,j} = \theta_{2n-1,i,j}$, $\theta_{2n,i,j} = \pi + \tilde{\theta}_{2n,i,j}$. In fields much weaker than spin-flip transition field β_2, one finds

$$\left|\tilde{\theta}_1(x,y,z) - \tilde{\theta}_2(x,y,z)\right| \ll 1 , \tag{43}$$

where $\tilde{\theta}_1(x,y,z)$ and $\tilde{\theta}_2(x,y,z)$ describe the direction of spins belonging to the first and second sublattices of the antiferromagnet, respectively.

Minimizing the total energy W over variables $\tilde{\theta}_{n,i,j}$ and moving to the continual representation in the resultant equations, we find in the bulk of the antiferromagnet, with regard for formula (43), that

$$\begin{aligned}\tilde{\theta}_2 - \tilde{\theta}_1 + \frac{1}{8}\,\Delta\tilde{\theta}_2 &= \alpha \sin 2\tilde{\theta}_1 + \beta \sin \tilde{\theta}_1\,,\\ \tilde{\theta}_1 - \tilde{\theta}_2 + \frac{1}{8}\,\Delta\tilde{\theta}_1 &= \alpha \sin 2\tilde{\theta}_2 - \beta \sin \tilde{\theta}_2\,,\end{aligned} \tag{44}$$

where Δ is the three-dimensional Laplacian in dimensionless variables $\xi = x/b_x$, $\eta = y/b_y$, $\zeta = z/b_z$, and $b_z = b_y$ is the size of a crystal tetragonal cell along the z-axis.

Introducing the variables

$$\theta = \frac{\tilde{\theta}_1 + \tilde{\theta}_2}{2}\,, \qquad \varphi = \tilde{\theta}_2 - \tilde{\theta}_1 \ll 1\,,$$

while adding and subtracting equations (44), leads to

$$\frac{1}{8}\,\Delta\theta = \alpha \sin 2\theta - \frac{1}{2}\,\beta\varphi \cos\theta\,, \tag{45}$$

$$\varphi + \frac{1}{16}\,\Delta\varphi = \beta \sin\theta\,. \tag{46}$$

We took into account in formulas (45) and (46) that $\alpha, \varphi \ll 1$ and neglected terms containing second and higher powers of these parameters.

When the size of magnetic inhomogeneities is much greater than the atomic size, $\Delta\varphi$ in equation (46) can be neglected. Then, it takes the form

$$\varphi = \beta \sin\theta\,. \tag{47}$$

Substituting the value of φ into formula (45), we arrive at

$$\Delta\theta = 2(\beta_1^2 - \beta^2)\sin 2\theta\,. \tag{48}$$

Let us consider now the situation at the antiferromagnet boundary. If the atomic plane belonging to the first sublattice is the upper one, a transition to the continual representation turns the equation for spin belonging to this plane into

$$\tilde{\theta}_2 - \tilde{\theta}_1 - \frac{1}{2}\,\frac{\partial\tilde{\theta}_2}{\partial\zeta} + \frac{1}{8}\,\Delta_{\xi,\eta}\tilde{\theta}_2 = 2\alpha \sin 2\tilde{\theta}_1 + 2\beta \sin\tilde{\theta}_1\,, \tag{49}$$

where $\Delta_{\xi,\eta}$ is the two-dimensional Laplacian in the layer plane. If the upper atomic plane belongs to the second sublattice, the boundary condition assumes the form

$$\tilde{\theta}_1 - \tilde{\theta}_2 - \frac{1}{2}\,\frac{\partial\tilde{\theta}_1}{\partial\zeta} + \frac{1}{8}\,\Delta_{\xi,\eta}\tilde{\theta}_1 = 2\alpha \sin 2\tilde{\theta}_2 - 2\beta \sin\tilde{\theta}_2\,. \tag{50}$$

Using the continuity of the function $\varphi(x, y, z)$, after passing to variables θ and φ and substituting formula (47) into Eqns (49), (50), we find

$$-\frac{1}{2}\,\frac{\partial\theta}{\partial\zeta} + \frac{1}{8}\,\Delta_{\xi,\eta}\theta = \pm\beta \sin\theta\,, \tag{51}$$

where the plus and minus signs on the right-hand side correspond to those cases in which the upper atomic plane belongs to the first or the second sublattices, respectively. On the opposite layer surface, the sign in front of derivative $\partial\theta/\partial\zeta$ in expression (51) must be changed.

Let us integrate Eqn (48) over the layer thickness, taking into account inequality $a \ll r_s$ and representing all terms with the exception of $\partial^2\theta/\partial\zeta^2$ as averaged-over-the-layer quantities. Integral $\partial^2\theta/\partial\zeta^2$ is calculated by the Newton–Leibniz formula using boundary conditions (51) to find $\partial\theta/\partial\zeta$ values at the layer boundaries. For odd M with the number of planes in the layer $M \gg 1$, it gives

$$\Delta_{\xi,\eta}\theta = \pm\frac{8\beta}{M}\sin\theta + 2(\beta_1^2 - \beta^2)\sin 2\theta\,. \tag{52}$$

The plus and minus signs correspond to the OA and OB regions, respectively.

For regions with even M, one obtains

$$\begin{aligned}\left.\frac{\partial\theta}{\partial\zeta}\right|_{\zeta=M/4} - \left.\frac{\partial\theta}{\partial\zeta}\right|_{\zeta=-M/4} &\approx \mp 2\beta\left(\sin\theta\big|_{\zeta=M/4} - \sin\theta\big|_{\zeta=-M/4}\right)\\ &\approx \mp\beta M\cos\theta\,\frac{\partial\theta}{\partial\zeta} \approx \beta^2 M\sin 2\theta\,.\end{aligned} \tag{53}$$

Averaging over layer thickness for the EA and EB regions leads to

$$\Delta_{\xi,\eta}\theta = 2(\beta_1^2 - 2\beta^2)\sin 2\theta\,. \tag{54}$$

The problem becomes one-dimensional in the case of a flat domain wall parallel to plane yz.

It is easy to see that the domain wall in the OA and OB regions, even in relatively weak fields $\beta_1 \gg \beta > (a/r_s)\beta_s$, has the thickness

$$\lambda_{\text{odd}} = b_x\left(\frac{M}{8\beta}\right)^{1/2}, \tag{55}$$

which is much smaller than both r_c and wall thickness λ_{even} in a region with an even number of atomic planes:

$$\lambda_{\text{even}} = \frac{b_x}{2\sqrt{|\beta_1^2 - 2\beta^2|}}\,. \tag{56}$$

Accordingly, the surface energy of such a wall is significantly higher; due to this, essentially the entire domain wall perpendicular to the layer surface, arising in the reorientation field at the boundary of the OB region, is in the region with an even number of atomic planes. When atomic step edges are parallel, the domain wall is located in the middle of the EA(EB) type region separating the OA and OB regions.

The thickness of a domain wall increases with growing magnetic field and tends to infinity as $(\beta_s - \beta)^{-1/2}$ in the surface spin-flop transition field, in contrast to the order parameter correlation radius that exhibits a similar trend in the bulk spin-flop transition field. As $\beta \to \beta_s$, the domain wall occupies the entire EA(EB) region; in fields stronger than the surface spin-flop transition field, it gradually transforms into two 90° domain walls at the region boundary (as shown in Fig. 3). In the center of the region, the spin-flop state considered in Section 3 is apparent.

If the EA(EB) region is enclosed between two OB regions, in reorientation field in the region as well as in adjacent regions the antiferromagnetic order parameter turns by 180°, no domain wall forms, and the EA type region turns into an EB one or vice versa.

A spin-flop transition in the EA(EB) region separating OA type regions is a first-order phase transition. Due to the interaction with the adjacent regions, the antiferromagnetism

vector in the center of the EA(EB) region changes jumpwise by a value smaller than $\pi/2$ and domain walls arise at its boundaries. As the magnetic field grows, the antiferromagnetism vector becomes oriented normally to it. The field β_s^* of this phase transition is higher than β_s and can be found from the condition $2\lambda(\beta_s^*) \approx R$. It follows from expression (56) that

$$\beta_s^* \approx \left[\beta_s^2 + \frac{1}{2}\left(\frac{b_x}{R}\right)^2\right]^{1/2}. \qquad (57)$$

Thus, a sequential series of events occurs in a weakly rough layer with the step width $R \gg r_s$ in parallel to magnetic field growth, viz. reorientation transition in OB type regions, spin-flop transition in EA(EB) regions, and spin-flop transition in OA type regions, respectively. These phase transitions will be somewhat blurred due to the mutual influence of regions of different types, their finiteness, and size differences.

5.1.2 $R \ll r_s$. As shown in Ref. [24], strong roughness precludes reorientation of certain OB type regions, while a spin-flop transition is realized in the entire layer volume.

Let us find the characteristic field of 'collective' spin-flop transition for $R \ll r_s$. To this effect, we shall consider a case in which the OA and OB regions occupy similar total areas σ_{OA} and σ_{OB} on the layer surface. Otherwise, the behavior of the system is dictated by the prevailing region type and consideration is analogous to that in the previous case but takes into account in the energy balance a factor equaling $(\sigma_{OA} - \sigma_{OB})/\sigma$, where σ is the total area of the layer surface.

Suppose that the antiferromagnetism vector averaged over the bulk of the layer makes an angle θ with the easy axis. In the OA and OB type regions, this vector additionally turns in different directions through the angle $\chi \ll 1$, so that magnetization of the extra (unpaired) atomic plane forms a minimal angle with the magnetic field direction. The resulting gain in the Zeeman energy is on the order of $\beta\chi b_x \sin\theta/a$ per cell, and the loss of the exchange energy for $R \gg a$ amounts approximately to $\chi^2 b_x^2/R^2$. Minimizing the total energy over χ, we find that $\chi \approx \beta R^2 \sin\theta/ab_x$ and a gain in total energy is of order $\beta^2 R^2 \sin^2\theta/a^2$ per cell. This gain in the spin-flop transition field must compensate for the energy loss $(\beta_1^2 - \beta^2)\sin^2\theta$ due to the spin flop phenomenon. Therefore, the spin-flop transition field is given by

$$\beta_{sf} \approx \beta_1 \frac{a}{R} \ll \beta_1 . \qquad (58)$$

It is easy to check that $\chi(\beta_{sf}) \ll 1$ and $\lambda_{odd}(\beta_{sf}) \gg R$ over the entire strong roughness region.

If $R \ll a$, the nonuniformity of the antiferromagnetic order parameter manifests itself only across the R-thick regions near each layer surface, the loss of the exchange energy is on the order of $\chi^2 b_x^2/Ra$, $\chi \approx \beta R b_x^{-1}\sin\theta$, and finally

$$\tau_{sf} \equiv 1 - \frac{\beta_{sf}}{\beta_1} \approx \beta_1 \frac{R}{a} \propto R, \qquad \tau_{sf} \ll 1 . \qquad (59)$$

The angle χ increases with the field growth and becomes on the order of unity at $\beta \approx \beta_0$. In the case of $\beta_0 \ll \beta_1^*$, equivalent to the condition $R \gg a$, the behavior of regions of different types in fields stronger than β_0 becomes 'individualized' and coincides with that considered in the preceding case. In the opposite limit, $R \ll a$, the system remains in the 'collective' spin-flop phase.

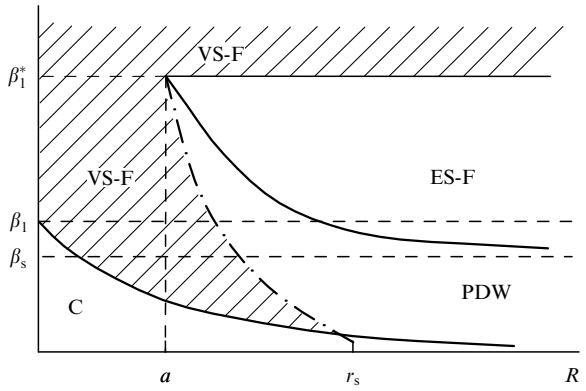

Figure 15. 'Magnetic field–roughness' phase diagram for a thin layer: C — collinear phase; PDW — phase with domain walls perpendicular to the layer surface and resulting from reorientation of OB type regions; ES-F — phase in which spin-flop transition occurs only in EB and EA type regions, and VS-F — bulk spin-flop phase. Solid curves are phase transition lines.

In fields $\beta \gg \beta_1^*$ which are weaker than the spin-flip transition field, when the correlation radius of the antiferromagnetic order parameter is $r_c \ll a$, the bulk of the layer is in the spin-flop phase and distortions of the order parameter near one of the layer surfaces do not affect those near the other. This regime has been considered in Section 4. Near the spin-flip transition field, roughness does not play any significant role and the size effect as $\beta \to \beta_2$ is similar to that described in Section 3.

The 'magnetic field–roughness' phase diagram for a thin antiferromagnetic layer is depicted in Fig. 15.

5.2 The thick layer

5.2.1 $a \gg R \gg r_s$. In this case, subdivision into surface domains occurs independently near each of the two layer boundaries in field β_s. Initial changes in the character of magnetic structure distortions in a growing magnetic field were described in Section 4. Correlation radius r_c increases as the field β strengthens and becomes equal to R in field β_R given by formula (38).

For $\beta > \beta_R$, a system of static vortices forms near each surface layer, which penetrate as deep inside it as approximately R; simultaneously, an r_c-thick 90° exchange spring arises parallel to the surface.

With a rise in the field strength, r_c increases and exchange springs occupy a progressively greater part of the layer. Simulation showed that in field β_a, when $2r_c(\beta_a) \approx a$, the middle part of the layer passes into the spin-flop phase as a result of the first-order phase transition. The β_a quantity is given by the relation

$$\tau_a \equiv 1 - \frac{\beta_a}{\beta_1} \approx \left(\frac{r_s}{a}\right)^2 . \qquad (60)$$

5.2.2 $a \gg r_s \gg R$. This case corresponds to the region of weak vortex distortions. As shown in Section 4, weak distortions and a 90° exchange spring develop near each layer surface in field $\tilde{\beta}_R$ [see formula (39)]. Then, a bulk spin-flop transition occurs in field β_a. Such a scenario is realized for $\tau_a < \tilde{\tau}_R$, which corresponds to the condition $aR > r_s^2$.

The scenario is different in the opposite case of $aR < r_s^2$. At a certain value of field $\tilde{\beta}$, the entire volume of the layer

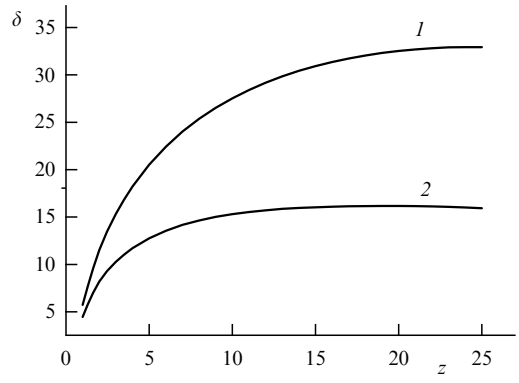

Figure 16. Domain wall thickness plotted vs. distances to interface for $r_s > a$ (curve *1*), and $r_s < a$ (curve *2*).

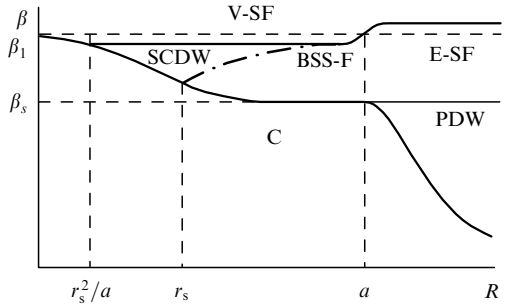

Figure 17. 'Magnetic field–roughness' phase diagram for a thick layer: BSS-F — phase with a surface spin-flop transition in type B regions, and SCDW — phase with surface 90° domain walls parallel to the layer; see Fig. 15 for the remaining notations.

passes instantaneously into the spin-flop phase with weak vortex distortions near the surface. The respective $\tilde{\tau}$ value is possible to estimate from the following line of reasoning: characteristic energy gain due to the appearance of weak distortions is of the same order of magnitude as Rb_x/r_s^2 per layer surface cell, while the loss (per layer surface cell) due to the formation of the spin-flop phase in a field weaker than the critical one β_1 is on the order of $(a/b_z)(\beta_1^2 - \beta^2) \approx ab_x\tilde{\tau}/r_s^2$. Hence it follows that

$$\tilde{\tau} \equiv 1 - \frac{\tilde{\beta}}{\beta_1} \approx \frac{R}{a}\,. \tag{61}$$

5.2.3 $\boldsymbol{R \gg a \gg r_s}$**.** In this case of weak surface roughness, the realizable scenario is analogous to that for $R \gg r_s$ for a thin layer; namely, a sequential series of events occurs as the magnetic field grows, including the reorientation transition in the OB type regions in field β_{reor} [see formula (42)], spin-flop transition in the EA(EB) type regions in field β_s, and a spin-flop transition in the OA type regions in field β_1^*. The following essential differences from the thin layer case need to be noted:

(1) In the EA(EB) type regions in field β_s, a 180° domain wall as thick as r_s and parallel to its boundaries arises in the center of the layer; it occupies only part of the layer thickness. To recall, the thin layer accommodated only the central part of the domain wall. As the field grows and approaches the value of the bulk spin-flop transition field, the wall overruns the entire layer thickness due to increasing r_c. This occurs in field β_a. While the field growth continues, the wall thickness does not increase further and remains finite as $\beta \to \beta_1$.

Let us turn to formula (48) to illustrate this scenario. In a one-dimensional case in the limit of $r_c \gg a$, Eqn (48) assumes the form $\theta''_{\zeta\zeta} = 0$, which suggests a linear dependence of the sublattice rotation angle in the bulk of the layer. Angle $\theta = \pi/2$ in the center of the layer changes by χ on approaching the layer surface, so that magnetization of the upper atomic plane makes an acute angle with the direction of the applied magnetic field. The value of χ is derived from the boundary condition (51): $\theta'_\zeta = \pm 2\beta \sin\theta$, which is transformed into the condition

$$\chi = \omega \cos\chi\,, \tag{62}$$

where $\omega = a\beta/b_z \approx a/\sqrt{2}\,r_s$. For $\omega \ll 1$, one has $\chi \approx \omega$, and for $\omega \gg 1$, relation $\chi \approx (\pi/2)(1 - \omega^{-1})$ is valid.

In fields $\beta > \beta_1$, the domain wall splits into two roughly 90° exchange springs localized near the layer surfaces.

(2) The domain wall perpendicular to the layer surface and separating regions with even and odd numbers of atomic planes in fields close to β_1 has the following structure: its width δ near the layer surface containing the edge of an atomic step is $\delta_0 \sim b_x/\beta$. The wall thickness increases linearly with the distance from the surface, with $d\delta/dz \sim 1$, and reaches the value of $\delta \approx \min(r_c, a)$. For $r_c < a$, the wall thickness does not change with further departure from the layer surface containing the atomic step. For $r_c > a$, the wall continues to thicken till it reaches the opposite layer surface (Fig. 16), and its energy per elementary cell length at the layer surface is estimated at $\ln(a/\delta_0)$ [22, 25].

The behavior of the system in fields $\beta \gg \beta_1^*$ is similar to that in the thin layer case. The 'magnetic field–roughness' phase diagram for a thick layer is demonstrated in Fig. 17.

To conclude, spin-flop transition in an antiferromagnetic nanolayer with uncompensated rough surfaces gives rise to a number of new types of domain walls whose thicknesses strongly depend on the magnetic field strength. Experimental observations of these walls is of great theoretical and applied interest.

6. Conclusion

We believe that this review provides convincing evidence that the physics of surface spin-flop transitions in antiferromagnets calls for further research; in particular, investigations into size effects in nanometer-scale antiferromagnetic specimens are far from complete.

The results of recent work already necessitate a revision of some seemingly settled views of the surface spin-flop transition and the resulting state, even though studies of this phenomenon for a real rough surface of antiferromagnet are only in their infancy.

This is especially true of experimental studies because the theory predicts a number of interesting objects, such as new types of domain walls arising from spin-flop transition in one part of a plane-parallel antiferromagnetic nanolayer and its absence in the other. Such unusual behavior of regions with an even and odd number of atomic planes parallel to the layer surfaces is of interest for both experimental investigations and possible practical applications. The width of these domain walls varies from a few dozen to hundreds of nanometers.

As mentioned above, modern magnetic microscopy techniques, such as magnetic-force, spin-polarization tunnel-

ing, and photoemission electron microscopies, make it possible to conduct relevant research and verify phase diagrams predicted in the review. We would like to wish success to our colleagues in this rather difficult work.

References

1. Néel L *Ann. Physique* **5** 232 (1936)
2. Berzin A A, Morosov A I, Sigov A S *Fiz. Tverd. Tela* **47** 1651 (2005) [*Phys. Solid State* **47** 1714 (2005)]
3. Mills D L *Phys. Rev. Lett.* **20** 18 (1968)
4. Mills D L, Saslow W M *Phys. Rev.* **171** 488 (1968)
5. Keffer F, Chow H *Phys. Rev. Lett.* **31** 1061 (1973)
6. Thompson S M *J. Phys. D* **41** 093001 (2008)
7. Fert A *Rev. Mod. Phys.* **80** 1517 (2008); *Usp. Fiz. Nauk* **178** 1336 (2008)
8. Grünberg P A *Rev. Mod. Phys.* **80** 1531 (2008); *Usp. Fiz. Nauk* **178** 1349 (2008)
9. Wang R W et al. *Phys. Rev. Lett.* **72** 920 (1994)
10. Trallori L *Phys. Rev. B* **57** 5923 (1998)
11. Papanicolaou N *J. Phys. Condens. Matter* **10** L131 (1998)
12. Dantas A L, Carriço A S *Phys. Rev. B* **59** 1223 (1999)
13. te Velthuis S G E et al. *Phys. Rev. Lett.* **89** 127203 (2002)
14. Bogdanov A N, Rößler U K *Phys. Rev. B* **68** 012407 (2003)
15. Rößler U K, Bogdanov A N *Phys. Rev. B* **69** 094405 (2004)
16. Rößler U K, Bogdanov A N *Phys. Rev. B* **69** 184420 (2004)
17. Lounis S, Dederichs P H, Blügel S *Phys. Rev. Lett.* **101** 107204 (2008)
18. Berzin A A, Morosov A I, Sigov A S *Fiz. Tverd. Tela* **52** 110 (2010) [*Phys. Solid State* **52** 117 (2010)]
19. Berzin A A, Morosov A I, Sigov A S *Fiz. Tverd. Tela* **47** 2009 (2005) [*Phys. Solid State* **47** 2095 (2005)]
20. Morosov A I, Morosov I A, Sigov A S *Fiz. Tverd. Tela* **48** 1798 (2006) [*Phys. Solid State* **48** 1909 (2006)]
21. Levchenko V D, Morosov A I, Sigov A S *Pis'ma Zh. Eksp. Teor. Fiz.* **71** 544 (2000) [*JETP Lett.* **71** 373 (2000)]
22. Morosov A I, Sigov A S *Fiz. Tverd. Tela* **46** 385 (2004) [*Phys. Solid State* **46** 395 (2004)]
23. Slonczewski J C *J. Magn. Magn. Mater.* **150** 13 (1995)
24. Morosov A I, Morosov I A, Sigov A S *Fiz. Tverd. Tela* **49** 1228 (2007) [*Phys. Solid State* **49** 1287 (2007)]
25. Levchenko V D et al. *Zh. Eksp. Teor. Fiz.* **114** 1817 (1998) [*JETP* **87** 985 (1998)]